

# **A Spectroradiometer for the Measurement of Direct and Scattered Solar Irradiance from on-board the NASA ER-2 High-altitude Research Aircraft**

C.T. McElroy

Atmospheric Environment Service, Downsview, Ontario, Canada

**Abstract:** A compact, diode-array spectrophotometer has been designed to make measurements of the downward spectral flux on a horizontal surface, the limb brightness and the apparent brightness in the nadir direction from on-board the NASA ER-2 research aircraft. The instrument was included as part of the photochemical payload used for the Stratospheric Photochemistry, Aerosol and Dynamics Expedition (SPADE) of the NASA High-Speed Research Program. The spectrophotometer is based on a 1024-element, randomly-addressable Reticon photodiode array and makes measurements covering the 300 to 775 nm spectral region at a resolution of about 1 nm. Some aspects of the design and the performance of the instrument during SPADE will be presented. The spectral measurements are in good agreement with modelled data (MODTRAN).

## **Introduction.**

A small, light-weight photodiode array spectrometer has been adapted to make measurements of the solar flux on a horizontal surface, the limb brightness and the apparent surface brightness below flight level from the NASA ER-2 high-altitude research aircraft as part of the Stratospheric Photochemistry, Aerosol and Dynamics Expedition (SPADE). The measurements are used to make a direct estimation of the J-values for significant photochemical reactions, to measure the apparent surface albedo below the aircraft, and to monitor the total ozone column above the aircraft. Eventually, trace gas concentrations at flight level will be retrieved from limb observations. Some spectrometric results from the SPADE measurement series will be presented here to demonstrate the instrument's performance. J-value results and a table listing measurement error contributions are included in a companion paper [McElroy et al., 1995] in this issue.

The NASA ER-2 has been used to make a number of widely publicized research expeditions to the Arctic [J. Geophys. Res., 1991] and the Antarctic [Geophys. Res. Lett., 1989] to study the chemistry and dynamics of the ozone layer, but flights have not included an instrument to measure the absolute spectral irradiance at flight level and estimate the diffuse component of the actinic flux.

The inclusion of the Composition and Photochemical Flux Measurement (CPFM) on the aircraft is designed to address two needs. One is for actual experimental measurements of stratospheric chemical composition and light flux levels. The other is to provide sensitive diagnostic information about the atmospheric light-scattering process to be used to verify the performance of the scattering models used for photochemical modelling purposes.

The practical difficulties associated with making measurements at all possible azimuth and elevation angles and at all wavelengths, coupled with the problem of handling the large data set which would result, lead to the selection of the particular

fields measured. These fields were selected to obtain a large information content in a data set of reasonable size and to meet the need for frequent estimates of the wavelength-dependent albedo under the aircraft track.

## The ER-2 Instrument

The spectrophotometer is based on an EG&G 1024-element, randomly-addressable photodiode array detector (#RL1024SRQ).

The detector is situated at the focus of an  $f/2$  holographic, diffraction grating made by American Holographic Inc. The instrument layout is shown in Figure 1. The design of the dispersing optics is such that a free spectral range of 375 to 775 nm, in the grating first order, is focused onto the array. The image of the entrance slit is equal to two detectors in width and leads to a measured spectral resolution with a full-width at half-maximum (FWHM) of about 1.2 nm in the first order.

A double filter-wheel assembly included in the spectrometer foreoptics allows for the introduction of a number of useful filter combinations. Appropriate band-limiting filters can be chosen to permit the use of the grating in either the first order (nominal wavelength range 375 to 775 nm) or in the second order (nominal wavelength range 188 to 388 nm). However, the declining UV sensitivity of the detector toward shorter wavelengths coupled with the passband of the UV11A order filter and the rapid attenuation of light in the atmosphere below the ozone layer at wavelengths less than 300 nm, means that data are only available down to about 300 nm. UV-transmitting film polarizers are included in one filter-wheel so that two orthogonal, linear polarization components of light from the limb can be measured. The polarizers block about 99% of the rejected plane of polarization and are 90% efficient at passing light polarized in the perpendicular direction.

The instrument is constructed of aluminum, for light weight, and the focus of the optics is temperature-compensated for use at an ambient temperature of about 10 degrees C during flight by using a detector mount made of plastic. The dimensions of the mount's components are designed to keep the detector at the focal plane of the grating as the instrument size changes with temperature. This means that there is a very small change with temperature of the instrument wavelength setting and dispersion, but the focal plane stays accurately in focus so that the slit function does not change with temperature. A change in focus degrades the slit function significantly for a small motion (e.g.: 0.001 inch, considering the  $f/2$  optics with a focal length of 1.8 inches), while the change in the dispersion is a small and correctable effect (much less than 0.1 nm; see Figure 3).

The foreoptics assembly includes a 1-inch focal length, UV achromat which provides a 0.1 degree by 10 degree field-of-view for the direct viewing directions (limb and nadir). The horizontal irradiance is measured by viewing a transmitting diffuser which approximates the performance of a cosine collector (see McElroy et al., 1995). The various fields-of-view and limb viewing angles are selected by rotating a 45-degree quartz directing prism using a stepping-motor drive. The pointing prism can also point at internal krypton and neon light sources which are focussed at infinity by individual lenses.

The detector has a very low dark current and it can be used

with integration times as long as 30 seconds. During the SPADE flights, integration times in the range 0.3 to 4 seconds were employed. Over this range of integration times and light levels the instrument/detector system absolute linearity has been tested to be better than 1%.

## **Payload Integration**

The CPFM instrument was integrated into the ER-2 payload by installing a wing pod containing the spectrometer, mounted inside an insulated cavity, at a pre-existing wing mounting-station. The pod has three viewing ports which allow a view of the nadir, the limb and the horizontal diffuser, which is mounted under a quartz dome.

In the initial planning for the experiment, there was concern that the white fuselage of the ER-2 would contribute a significant signal to the horizontal diffuser. However, the fuselage is only about 1 m by 10 m and is situated more than 12 m away from the instrument mounting location. If the aircraft is assumed to be a Lambertian surface with an albedo of 1, then the light contribution to the horizontal diffuser is less than 10% for relative solar zenith angles of less than 80 degrees and less than 2% for angles less than 45 degrees when the cosine effects for both signals are included.

The possible effects of wing motion at the instrument mounting station were investigated using gravitationally-driven, rotation sensors in both the pitch and roll directions to quantify wing motions. As a result, the data processing for SPADE includes a 4.5 degree 'static' angle shift (relative to the ground survey), but does not account for smaller drifts throughout the flight. The latter will eventually be included as well, so that the reported limb-viewing angles will be known to higher accuracy.

A '386, single-board computer with 50 megabytes of 'flash' (electrically alterable) memory is mounted in the electronics bay of the aircraft and accepts data from the instrument via the aircraft wiring harness. Navigational data are also recorded in the spectral data blocks. These data are used in the post-flight analysis to determine the aircraft position and altitude in order to calculate the solar zenith angle, azimuth angle and angle relative to the instrument diffuser normal. The static angles which the various reference directions of the pod make with respect to the navigation system were carefully surveyed (<0.05 degrees).

## **Instrument Noise Level**

An analysis of the electronic circuitry in the spectrophotometer shows that the sensitivity of the digitizing electronics is approximately 1300 electrons per A/D count. The observed dark count of about 1500 bits per second translates to a dark current at the detector of about 2 million electrons for a 1-second integration time. The manufacturer's specification [EG&G Reticon, 1991] of 0.5 pA per detector at 25 degrees C is in good agreement with this number. The shot noise associated with this dark current is one A/D count.

The video line of the Reticon detector is read twice for each output point, once after being reset but with zero integration time

and then once after reset and the selected measurement integration time. The difference between these readings is the measure of the incident light. This algorithm provides compensation of analog offset drift and of video-line offsets generated by very high light levels. Because the video line is read twice, the intrinsic, random electrical noise contributes twice to the final noise level of the output signal. The sum of all of these noise components is 2 to 3 A/D counts as illustrated in the ratio curve in Figure 4, which also includes contributions from the aircraft attitude information. The calibration process also introduces an absolute error contribution from the noise in the additional measurements used to create the instrument responsivity curve. The noise increases because of decreased responsivity toward longer wavelengths and around the 350 to 400 nm region where the transition between first- and second-order data takes place.

The mean dark count level of pixels in the (nominal) 227 to 267 nm range in the second order, which are dark because of the combined filtering effect of the atmosphere and the instrument order filter (FWHM: 305 - 373 nm), is used as a measure of the detector temperature. The log of the dark count from each pixel at each integration time used is fitted using a linear regression to the log of the mean dark count of the dark pixels.

For each block of data analyzed, the calculated log of the dark pixel mean (the proxy measure of temperature) is determined and used to estimate the dark spectrum to be subtracted from each observation. In the case of the UV spectra, the dark spectrum is further scaled by the ratio of the actual dark pixel mean to the mean of the predicted dark pixels. The accuracy of the dark spectrum correction is particularly significant for the UV spectra where the intensity levels are low and the sensitivity of the detection system is falling toward shorter wavelengths. It is also important in the near-UV part of the visible order where the band-limiting filter causes the instrument throughput to drop.

If some stray-light signal is included (mistakenly) as dark count, the scaling of the dark count in this way simply provides a small amount of 'correction' for the stray light. Tests done to detect this have shown the effect to be negligible, implying that the majority of the stray light in the instrument is 'nearby' stray light which is significant in the 300 nm region.

## **Stray Light**

While detailed testing of the instrument spatial stray light characteristics has not yet been done, simple tests done in the laboratory and scanning across the sun from space have shown that the rejection of off-axis light is at least on the order of 100:1. Since the measurements made on the limb are currently only being used to determine the maximum value of the limb brightness, for the purpose of estimating J-values, there will be no significant error associated with stray light in the foreoptics.

Internally scattered light in the spectrometer is another matter.

The use of an order filter which restricts the light entering the instrument to a band between 295 and 390 nm greatly reduces the total energy at longer wavelengths which can be scattered inside the instrument. But because of the sharp cutoff of the solar spectrum by ozone at wavelengths shorter than 310 nm, stray light in the instrument becomes detectable in that region.

The stray light contribution is corrected by assuming that there

is no real light signal contribution from sunlight or scattered light in the atmosphere (below the ozone layer) between 290 and 295 nm and that the stray light signal changes slowly with wavelength. The mean signal produced by photodiodes at these nominal wavelengths is subtracted from the signal from all other photodiodes. Because the real signal increases very rapidly toward longer wavelengths (within a few nanometres the correction is not significant) this method provides a very good correction [Kerr and McElroy, 1993]. Stray light contributes about 60% of the observed signal at 300 nm, drops to about 15% by 303 nm and contributes less than 2% at 305 nm.

## **Instrument Calibration**

The spectrophotometer's absolute spectral responsivity is calibrated by exposing the horizontal diffuser to light from a DXW-type quartz-halogen lamp whose calibration by the vendor (Optronics Laboratories, Inc.) is traceable to the United States National Institute for Standards and Technology (NIST). The lamp's calibration certificate is warranted accurate to better than 2% over the wavelength range 300 to 800 nm.

The direct-viewing ports (limb and nadir) are calibrated by making observations of the surface radiance of a Spectralon diffuser which is illuminated by the calibrated, quartz-halogen lamp. The diffuser was provided, together with a calibration certificate, by the manufacturer: Labsphere, Inc. It is assumed that the radiation scattered from the diffuse surface is distributed according to the Lambertian law of diffuse reflection so that the surface brightness is given as:  $I_s = F / \pi$ , where  $I_s$  is surface brightness and  $F$  is the lamp flux onto the surface. To minimize the contribution to the total calibration error from departures from perfect Lambertian behaviour, the surface is illuminated and viewed from as nearly a normal direction as is practical.

The calibration process was repeated in the field as frequently as flight operations permitted, including before the first flight and after the last. As much as possible, the instrument was left undisturbed in the aircraft wing pod and the pod assembly transported to and from the laboratory area intact so as to minimize the chances that the calibration process would cause changes in the system sensitivity.

The wavelengths of the spectral elements measured are computed using a cubic dispersion equation which associates a wavelength with each Reticon detector element. The coefficients of the equation are determined by viewing mercury and neon emission lines. During the flight observation sequence, periodic measurements of the spectrum of an internal neon lamp are used to track small temperature- and pressure-induced wavelength shifts. The wavelength of light changes at altitude because the index of refraction of a gas is proportional to its number density, while the velocity of light is inversely proportional to the refractive index. The apparent wavelengths of specific absorption lines will change with the instrument ambient pressure.

The calibrated fluxes and intensities determined from the instrument observations are calculated by scaling the instrument response as a function of wavelength during the measurement flights by the values produced by the instrument while observing

calibrated sources. The details of the data reduction steps and a table listing the various errors in the reduced data are included in the companion paper by McElroy et al. [1995] in this issue.

## Results

Spectra have been analyzed and compared to help establish, objectively, the precision and accuracy of the data collected. Figure 3 shows the variation in the apparent position of a neon reference line and a Fraunhofer solar absorption feature during the flight. Part of the variation is due to the pressure change as the aircraft goes to higher altitudes and the rest is from differential temperature effects. Spectra taken at flight altitude approximately 2 seconds apart are shown as Figure 4 to illustrate the instrument signal-to-noise characteristics. The difference curve clearly illustrates that the signal-to-noise ratio is 100:1 or better.

The discontinuity in the difference curve near 375 nm is where the UV and visible spectra are blended to produce the composite spectrum. The two spectra are measured 2 seconds apart. The size of the UV error is larger because of the lower signal and instrument throughput, and is of opposite sign from the difference in the visible portion. The change of sign is not significant.

Figures 5 and 6 compare an observed solar spectrum collected on May 12, 1993 with one calculated by the MODTRAN atmospheric transmission model [MODTRAN, 1993]. The model run was done with background stratospheric aerosol and high volcanic aerosol selected, and using a climatological ozone profile. The calculation was made for the aircraft altitude and for the solar zenith angle at the time the CPFM spectrum was measured. The small differences between the MODTRAN and CPFM results (about 5%) at longer wavelengths (550 to 775 nm) is partly due to errors in the cosine response correction, which has a wavelength dependence. The larger difference in the UV (about 20%) may be because the aerosol properties of the atmosphere were not well represented by the aerosol model in MODTRAN, nor was the actual ozone profile present on the day of the observations used. Figure 5 shows that, even when the sun is high in the sky, the spectral irradiance changes by about two orders of magnitude over the 10 nm between 300 and 310 nm.

**Acknowledgements.** The author would like to acknowledge the contributions of a number of people. Clive Midwinter, Robert Hall, David Barton, Aaron Ullberg, Steve Werchohlad and Ed Vala of the AES laboured long and hard to take the CPFM concept to operational status in only 4 months. This effort would not have succeeded without the encouragement and outstanding co-operation of Lockheed Corporation, the aircraft engineering support contractor, and the NASA/Ames personnel who are responsible for the management of the ER-2 program. The author is pleased to acknowledge the useful comments and suggestions of the referees.

## References

EG&G Reticon, Image Sensing Product Catalog #055-0261, p. 63, September, 1991.

*Geophys. Res. Lett.*, Special Issue, 17, 1990.

*J. Geophys. Res.*, Special Issue, 14, 1989.

Kerr, J.B., and C.T. McElroy, Evidence for large upward trends of ultraviolet-B radiation linked to ozone depletion, *Science*, 1032-1034, 1993.

McElroy, C.T., C. Midwinter, D.V. Barton, and R.B. Hall, A comparison of J-values estimated by the Composition and Photodissociative Flux Measurement with model calculations, *Geophys. Res. Lett.*, this issue, 1994.

MODTRAN 2, Oncore software manual, Pub. Ontar corp., North Andover MA, 1993.

C.T. McElroy, Atmospheric Environment Service,  
4905 Dufferin Street, Downsview, Ontario, M3H 5T4  
(e-mail: [tmcelroy@dow.on.doe.ca](mailto:tmcelroy@dow.on.doe.ca))

McELROY: NASA ER-2 AIRCRAFT SPECTRORADIOMETER

**Figure 1.** Spectrometer optical arrangement.

**Figure 2.** CPFM spectrophotometer installation in the ER-2 wing pod.

**Figure 3.** The position of selected neon and Fraunhofer reference lines as a function of time in thousands of seconds from midnight U.T.C. of the flight day.

**Figure 4.** Cosine-corrected spectra taken two minutes apart on May 14 are compared. Both spectra and their difference are included in the plot.

**Figure 5.** May 12, 1993 measurements are compared with a calculation done using MODTRAN. The ozone column amount used in the calculation was not exactly matched to the amount measured (320 DU) above the aircraft. The observations were taken at 23:04 U.T.C. at an altitude of 18.5 km and a solar zenith angle of 42.8 degrees.

**Figure 6.** As in Figure 5, but for the full range 300 - 775 nm. The difference between MODTRAN and the observations is about 5% for most of the spectrum.

**Figure 1.** Spectrometer optical arrangement.

**Figure 2.** The position of selected neon and Fraunhofer reference lines as a function of time in thousands of seconds from midnight U.T.C. of the flight day.

**Figure 3.** Cosine-corrected spectra taken two minutes apart on May 14 are compared. Both spectra and their difference are included in the plot.

**Figure 4.** May 12, 1993 measurements are compared with a calculation done using MODTRAN. The ozone column amount used in the calculation was not exactly matched to the amount measured (320 DU) above the aircraft. The observations were taken at 23:04 U.T.C. at an altitude of 18.5 km and a solar zenith angle of 42.8 degrees.

**Figure 5.** As in Figure 4, but for the full range 300 - 775 nm. The difference between MODTRAN and the observations is about 5% for most of the spectrum.



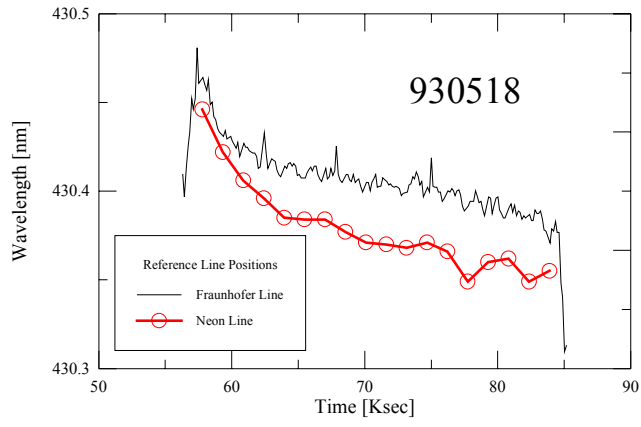


Figure 2

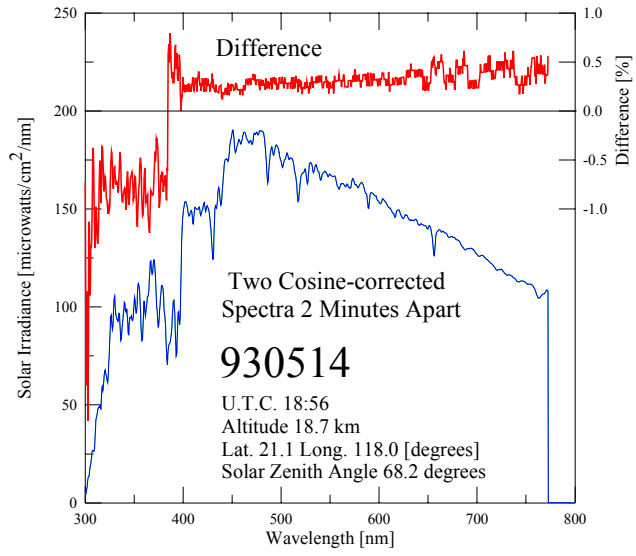


Figure 3

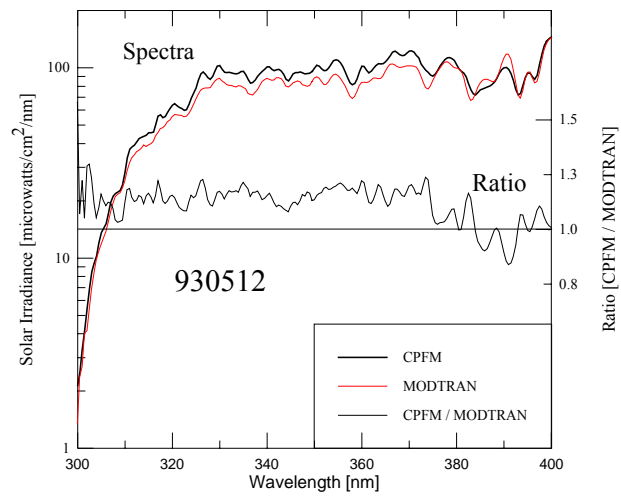


Figure 4

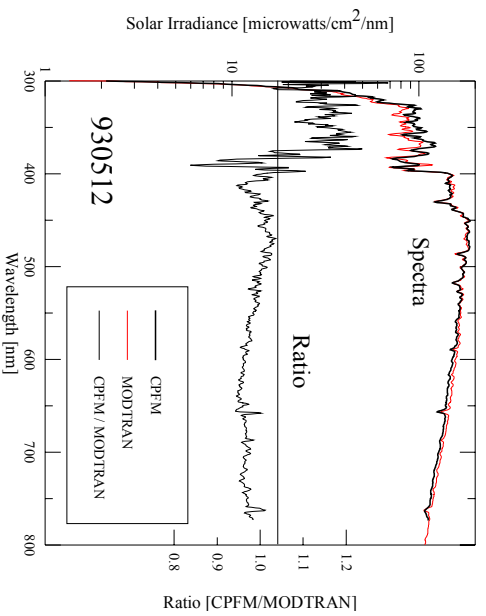


Figure 5